Volume 11, No. 1, 2022, pp. 91-103
Academy of Romanian Scientists Online ISSN 2285 – 4177
Annals Series on Biological Sciences ORIGINAL PAPERS

Insulin Resistance and the Metabolic Syndrome Severity – a Mathematical Model

Elizabeth KERTOWIDJOJO[1], Dumitru Andrei IACOBAŞ[2,3,4]

[1] Assistant Professor, MD, PhD, Department of Pathology, University of Chicago, Chicago, IL 60637, U.S.A.
[2]Research Professor, PhD. Director Personalized Genomics Laboratory, Center for Computational Systems Biology, Prairie View A&M University, Prairie View, TX 77407, U.S.A. (daiacobas@pvamu.edu)
[3] Professor Emeritus, "Ovidius" University, Constanta
[4] Honorary Member, Academy of Romanian Scientists

Abstract. *Excessive fructose consumption was shown to have deleterious effects on the cardiovascular system, particularly as the metabolic syndrome. However, the degree by which alteration of each pathophysiological factor contributes to the morbidity associated with fructose consumption is not yet clear. We have developed a mathematical model to integrate and uniformly quantify pathophysiological features of the metabolic syndrome on a high fructose-fed dog model. A novel comprehensive measure for the syndrome severity (the "patholog") and a more intuitive measure of the insulin resistance are introduced. Alteration of hemodynamics, echocardiography and blood chemistry were determined in adult male mongrel dogs fed with 60% isocaloric fructose or normal chow for 7 weeks. The diverse experimental data were transformed into comparable scores and a pre-Hilbert space of states constructed. In such a space one can quantify the severity of any combination of pathophysiological and genomic features and determine the global recovery resulting from a treatment. The model indicates increase of insulin resistance (new index proposed), systolic blood pressure, low-to-high density lipids ratio and angiotensin II as the major contributors to the excessive fructose morbidity. Our model provides the simplest, yet the most intuitive and comprehensive way to integrate data of a wide diversity in visualizing and quantifying a cardiovascular disease.*

Key words: Fructose consumption, Cholesterol, Insulin resistance, Angiotensin II, Dog model

DOI https://doi.org/10.56082/annalsarscibio.2022.1.91

1. Introduction

One major cause of obesity, type 2 diabetes, fatty liver and cardiovascular disease of millions in the Western world countries is the excessive sugar consumption, particularly in the form of high-fructose corn syrup [1-4]. Such consequences of the excessive fructose consumption are heralded by the metabolic syndrome [5-9], a combination of medical disorders reaching a prevalence of 35-39% in the United States [10]. According to the American Heart Association, the metabolic syndrome is characterized by: 1) increased waist circumference (men > 102 cm, women >90 cm), 2) elevated triglycerides (≥150 mg/dL), 3) reduced high density lipids (men < 40 mg/dL, women (< 50 mg/dL), 4) elevated blood pressure (≥ 130/85 mmHg), 5) elevated fasting glucose (≥ 100 mg/dL)1. High fructose diet results in hypertension [11], atherosclerosis [12], hyperurecimia [13],

endothelial dysregulation [14], dyslipidemia [15,16] consistent with the metabolic syndrome.

Fructose is a monosaccharide naturally found in many fruits and vegetables. A major dietary source comes from the high-fructose corn syrup commonly added processed foods such as soft drinks, condiments, applesauce and even baby food [17]. In contrast to glucose which is metabolized in many organs, fructose is solely metabolized in the liver. Fructose metabolism bypasses phosphofructokinase in glycolysis and is not affected by insulin. Fructose actually induces insulin resistance [18-20], leading to a higher caloric intake by reducing the level of circulating leptin [21-23].

2. Materials and methods

This report reanalyzes from a novel perspective the experimental data on fructose-fed dogs included in the PhD thesis of Dr. Kertowidjojo. Experimental protocols were approved by the Institutional Animal Care and Use Committee and respected the guidelines of the National Institutes of Health and the American Physiological Society.

2.1. Animals

Six adult mongrel male dogs were fed for seven weeks with 60% isocaloric fructose. Time 0 was considered as control (baseline) for each dog, providing the best reference for the progression of the metabolic syndrome.

2.2. Hemodynamics

Hemodynamic measurements were recorded in the conscious state using implanted instruments as previously described [24-27]. Coronary blood flow (**CBF**) and mean coronary flow (**MCF**) were determined with a Doppler flow transducer placed on the left circumflex coronary artery. The left ventricle was monitored for systolic (**SBP**) and diastolic blood pressure (**DBP**), mean arterial pressure (**MAP**) and end-diastolic (**LVEP**) pressure. The rate of the left ventricle pressure rise (**dP/dt**) was obtained with an operational amplifier (National Semiconductor LM 324).

2.3. Echocardiography

Echocardiography was performed with an Acusan 356 Sequoia in both a longitudinal and M-mode view [28] to determine the heart rate (**HR**), stroke volume (**SV**) and left ventricle diameter in diastole (**LVDD**) and systole (**LVDS**). Cardiac output (**CO** = HR x SV), fractional shortening (**FS** = (1-LVDS/LVDD)x100%), coronary vascular resistance (**CVR** = MAP/CBF) and total peripheral resistance (**TPR** = MAP/CO) were considered instead of the independent variables used to calculate them.

2.4. Blood chemistry

Blood samples were taken from an implanted catheter. Plasma insulin (**INS**), angiotensin II (**ANG**), uric acid (**UA**), homocysteine (**HC**), and high (**HDL**) and low (**LDL**) density lipids were measured as previously described [29].

2.5. Glucose tolerance test and insulin resistance

In addition to dosing blood levels of glucose (**GLU**) and INS, we performed an intravenous glucose tolerance test in the morning, after 12 hours of fasting at baseline, 4 and 7 weeks on fructose. Insulin resistance IR was defined as the insulin level [*INS*] multiplied by the time necessary to reduce the glucose concentration at half, denoted as $T_{1/2}$. In normal conditions, increase of insulin level reduces $T_{1/2}$.

$$IR = [INS]T_{1/2} \quad (1)$$

2.6. Data transformation

Pathophysiological characteristics are of diverse nature, expressed in different units and bear unequal importance for the system, making difficult their integration into functional models. For instance, has 20% increase of SBP equivalent effects on the cardiovascular system as 20% increase of INS level, 20% increase of LDL or 20% increase of TPR?

In order to make the alterations comparable, we transformed the real feature *i* values for dog δ after *w* (= 0,1,2,3,4,5,6,7) fructose-feeding weeks, $\alpha_i^{(\delta,w)}$ into numbers. First, we referred each feature α of each dog δ at each time point *w* (weeks fructose feeding) to its baseline (self- reference to normalize the biological variability). Then we determined the mean and standard deviation for all dogs at the same time point.

$$\beta_i^{(\delta.w)} \equiv \left(\frac{\alpha_i^{(\delta,w)}}{\alpha_i^{(\delta,0)}} \right) \quad , \quad a_i^{(w)} = \left\langle \beta_i^{(\delta,w)} \right\rangle_{\text{all } \delta} \Rightarrow a_i^{(0)} = 1$$

$$s_i^{(w)} = \begin{cases} \dfrac{\varepsilon_i^{(0)}}{\left\langle \alpha_i^{(\delta,0)} \right\rangle_{\text{all } \delta}} & if \quad w = 0 \\ stdev \left\langle \beta_i^{(\delta,w)} \right\rangle_{\text{all } \delta} & if \quad w > 0 \end{cases} \tag{2}$$

To each feature *i* at each time point *w* we assigned the standard numerical score:

$$\zeta_i^{(w)} \equiv \frac{a_i^{(w)} - 1}{s_i^{(w)}} \Rightarrow \zeta_i^{(0)} = 0 \tag{3}$$

In transformation (3) we have implicitly assumed that the ratio-to-physiological feature values are from (or could be approximated with) a normal or a lognormal distribution [30] of possibilities. The lognormal distribution is a continuous probability distribution of a random variable whose logarithm is normally distributed. Almost all pathophysiological features spanning the entire axis of real numbers are normally distributed and almost all non-negative features are lognormally distributed. All features used in this report are lognormally distributed. The standard scoring (3) makes all lognormally distributed features comparable. Thus, a 20% increase of ζ (but not of α) means the same deviation from normal, regardless the nature of that feature.

2.7. Significant regulation

A feature was considered as significantly regulated after *w* weeks of fructose feeding with respect to control if the composite criterion (4) is satisfied:

$$\left| \zeta_i^{(w)} \right| > \underset{cut-off}{\xi_i^{(w)}} \equiv 1 + \underbrace{\sqrt{2\left(\left(\frac{s_i^{(w)}}{a_i^{(w)}} \right)^2 + \left(\frac{s_i^{(0)}}{a_i^{(0)}} \right)^2 \right)}}_{\text{pooled coefficient of variation}} \quad \wedge$$

$$p_{val}\left(\underbrace{ttest\left(\left\{ \alpha_i^{(\delta;w)} \right\}, \left\{ \alpha_i^{(\delta;w)} \right\}, 2, 3 \right)_{\text{all } \delta}}_{\text{heteroscedastic t-test of means equality}} \right) < 0.05 \tag{4}$$

Criterion (4) requires that the absolute ζ score exceeds the cut-off ξ determined for that feature in that condition, AND the p-val of the heteroscedastic *t*-test for the equality of distributions' means [31] is less than 0.05. The cut-off incorporates the technical noise and biological variability in both compared conditions (0 and *w* weeks of fructose feeding).

2.8. Correlation of the pathophysiological characteristics

One may consider the blood and the left ventricle of each of the six dogs, at each time point, as of one generic dog tuned to adapt six slightly different (not significantly regulating) local environments. Therefore, we have used Pearson product-moment correlation coefficient to determine the degree by which dog–to-dog variability in one feature is correlated to variability in each other feature in the same condition. Pearson correlation indicates whether the two features are linearly related. Also, we have determined the correlation between the profiles of two features for the same dog during the fructose feeding and averaged the results for the six dogs. In both cases, close to unit positive/negative values indicate synergistic/antagonistic expression, while close to zero values indicate independence of the considered features. The cut-off value of the coefficient of correlation between two features to be considered as synergistically/ antagonistically/independently expressed was determined for each feature pair by taking into account the effect of the inherent technical noise on those features [32]. However, only the correlation of dog-to-dog variation of two features in the same condition (# weeks of fructose feeding) indicates that such features may regulate each-other. Correlation between changes of two features during the seven-week experiment indicates only that a common factor (here fructose feeding) regulates both.

2.9. The pre-Hilbert space of states and the "Patholog" of a state

For quantitative evaluation of the fructose feeding effects, the model variables *z* are expressed to take positive/negative values for statistically significant up-/down-regulation, 0-value indicating no regulation:

$$z_i^{(w)} = \begin{cases} \dfrac{\zeta_i^{(w)}}{\left|\zeta_i^{(w)}\right|}\left(\left|\zeta_i^{(w)}\right| - \xi_i^{(w)}\right) & if \quad \left|\zeta_i^{(w)}\right| > \xi_i^{(w)} \wedge p_{val} < 0.05 \\ 0 & if \qquad else \end{cases} \tag{5}$$

Using the *z*-scores one can build the pre-Hilbert space (norm derived from a scalar product) of states having as many dimensions (*N*) as independent features are considered from the perspective of Pearson correlation coefficient. In this space, each point represents a possible state and each curve a possible evolution. As constructed, the central point (all coordinates are 0) is the control state (here before starting the fructose diet). Given the independence and the way we normalize the features the space is orthonormal and the multi-dimensional Pythagoras' theorem can be applied. Therefore, we define the "**patholog**" (*sic!*) Ψ of a state with respect to a subset Φ of features (e.g. blood hormones) as the Euclidian distance to the control state [33, 34].

$$\Psi^{(w)}(\Phi) = \sqrt{\sum_{i\in\Phi}\left(z_i^{(w)}\right)^2} \tag{6}$$

As defined, the "patholog" incorporates alterations of all quantified features in the selected subset. Since the feature subsets could be of different sizes (e.g.: 5 hemodynamics vs 2 lipids) we defined and used the "standard patholog" Π

$$\Pi \equiv \sqrt{\left\langle \left(z_i^{(w)} \right)^2 \right\rangle} \qquad (7)$$

to compare the alterations of subsets of various sizes.

2.10. Data processing

OriginPro 8.5, GraphPad Prism 9 and Excel (Office 2020) were used for data analysis and graphs.

3. Results and discussions

3.1. Insulin resistance

Figure 1 shows that insulin level and half-life in the glucose tolerance test are inversely correlated at the base line, justifying our IR index. Thus, normally fed dogs with higher insulin level metabolize faster (smaller half-life) the injected glucose than dogs with lower insulin levels.

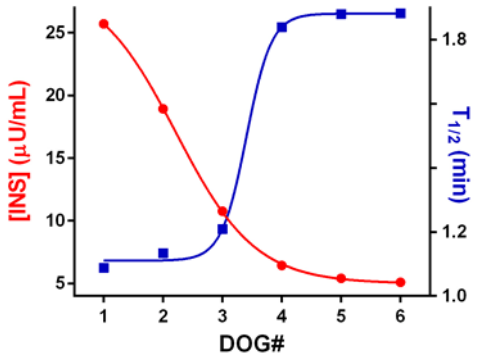

Fig. 1. Insulin level [INS] and half-life $T_{1/2}$ in glucose tolerance test of normally fed dogs.

The dogs were ordered with respect to decreasing [INS]. Experimental data were fitted with sigmoidal functions only to show that a decrease in the insulin level is accompanied by an increase of the glucose half-life (no relationship between dog number and [INS] or $T_{1/2}$).

As presented in Fig. 2A, insulin level of high fructose-fed dogs increases exponentially (e.g. 3.4x after 4 weeks and 7.2x after 7 weeks) without exhibiting saturation during this period. The exponential growth constants were obtained using GraphPad Prism:

$$INS(t) = INS(0)e^{kt} \quad \Rightarrow \quad INS(w) = (10.47 \pm 1.82)e^{(0.303 \pm 0.030)w}$$

However, instead of the expected faster glucose decay we found a substantially slower one, taking longer to reduce glucose concentration to half (i.e. larger half-life $T_{1/2}$, Fig. 2B). Experimental data were fitted with one phase decay law, with the decay rate K and $[glu]_0$ and $[glu]_\infty$ the initial (1 min after injection) and residual (at the end of the test) glucose levels:

$$[glu]_t = \left([glu]_0 - [glu]_\infty \right) e^{-Kt} + [glu]_\infty \quad , \quad half-life\ T_{1/2} = \frac{\ln 2}{K}$$

We found that *IR* increased faster than the insulin level (9.8x and 30.5x for IR vs 3.4x and 7.2x for [INS]) . These results confirm the fructose-feeding induced insulin resistance syndrome [19, 35-39]. Using the above-defined IR measure, *the insulin resistance increased by 9.75x after 4 weeks and by 30.45x after 7 weeks of fructose feeding* (Fig. 2C).

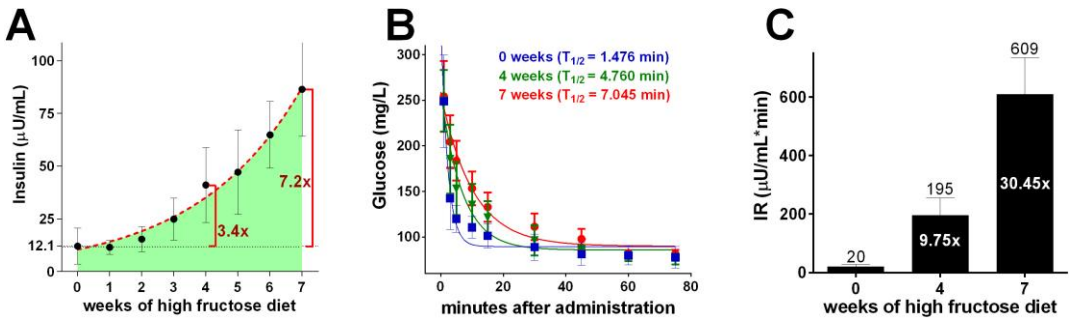

Fig.2. Insulin level, glucose tolerance test and insulin resistance. A. Increase of plasma insulin level during high fructose feeding. B. Glucose test in 6 adult male dogs after 0, 4 and 7 weeks of fructose feeding. C. Increase of insulin resistance (IR).

3.2. Alteration of hemodynamics, echocardiography, blood chemistry and lipids

Figure 3 presents the evolution of several characteristics during high fructose diet. The absolute values were ζ-transformed to make comparable the severity of their alteration as illustrated in Table 1 for SBP and INS.

		α1	α2	α3	α4	α5	α6	AVERAGE	STDEV	β1	β2	β3	β4	β5	β6	a	ζ	s	ξ	z
SBP	Baseline	125	120	125	120	120	130	123.33	4.08	1.00	1.00	1.00	1.00	1.00	1.00	1.00	0.00	0.03		0.00
	Week 1	130	110	120	125	100	135	120.00	13.04	1.04	0.92	0.96	1.04	0.83	1.04	0.97	1.01	0.09	1.13	0.00
	Week 2	120	110	125	125	125	130	122.50	6.89	0.96	0.92	1.00	1.04	1.04	1.00	0.99	-0.20	0.05	1.08	0.00
	Week 3	125	120	130	140	140	130	130.83	8.01	1.00	1.00	1.04	1.17	1.17	1.00	1.06	1.88	0.08	1.12	0.00
	Week 4	135	150	120	140	145	135	137.50	10.37	1.08	1.25	0.96	1.17	1.21	1.04	1.12	3.54	0.11	1.15	2.40
	Week 5	140	160	135	140	150	140	144.17	9.17	1.12	1.33	1.08	1.17	1.25	1.08	1.17	5.17	0.10	1.13	4.04
	Week 6	150	160	140	160	150	145	150.83	8.01	1.20	1.33	1.12	1.33	1.25	1.12	1.23	6.81	0.10	1.12	5.69
	Week 7	150	155	160	165	160	155	157.50	5.24	1.20	1.29	1.28	1.38	1.33	1.19	1.28	8.42	0.07	1.09	7.33
INS	Baseline	5.41	6.45	5.09	18.9	25.7	10.8	12.06	8.47	1.00	1.00	1.00	1.00	1.00	1.00	1.00	0.00	0.70		0.00
	Week 1	7.8	7.73	14.7	15	13.3	10.7	11.53	3.29	1.44	1.20	2.88	0.79	0.52	0.99	1.30	0.43	0.84	2.34	0.00
	Week 2	11.8	7.02	23.2	12.8	20.4	17.1	15.38	5.98	2.19	1.09	4.56	0.67	0.79	1.59	1.81	1.16	1.45	2.50	0.00
	Week 3	26.9	13.9	41.9	16.6	27.1	22.8	24.87	9.92	4.98	2.16	8.23	0.88	1.05	2.12	3.24	3.18	2.85	2.59	0.59
	Week 4	31.2	23.8	66.8	27.8	59.3	37.4	41.05	17.75	5.77	3.70	13.11	1.47	2.31	3.48	4.97	5.65	4.25	2.56	3.09
	Week 5	40.2	29.4	44.4	36.2	86.1	46.5	47.13	20.03	7.43	4.56	8.72	1.91	3.35	4.32	5.05	5.76	2.56	2.22	3.54
	Week 6	75	39.7	85.3	55.8	65.7	67.3	64.80	15.77	13.85	6.16	16.76	2.95	2.56	6.25	8.09	10.08	5.88	2.43	7.66
	Week 7	118	78.9	65.2	72.6	72.8	111	86.42	22.29	21.82	12.24	12.81	3.84	2.83	10.30	10.64	13.71	6.92	2.35	11.36

Table 1. Systolic Blood Pressure (SBP) and Insulin level (INS) real data and their transformation. Red background in column z indicates significant up-regulation.

Note the significant increase of insulin (INS) and angiotensin II (ANG II) after 3 weeks and of "bad cholesterol" (LDL) and systolic blood pressure (SBS) after 4 weeks of high fructose feeding. Decrease of "good cholesterol" (HDL) and increase of homocystein (HC) and uric acid (UA) became significant after 5 weeks and increase of

diastolic blood pressure (DBP) after 6 weeks. The alterations continue to develop and the left ventricle end-diastolic (LVEP) pressure, coronary vascular (CVR) and total peripheral (TPR) changed significantly after 7 weeks. The heart rate, cardiac output, rate of left ventricle pressure rise, left ventricle diameter in systole/ diastole and the mean coronary flow were not significantly altered even after 7 weeks fructose. Interestingly, alteration of low-to high density lipids ratio (LDL/HDL) became significant after 2 weeks although the LDL changed significantly after 4 and HDL after 5.

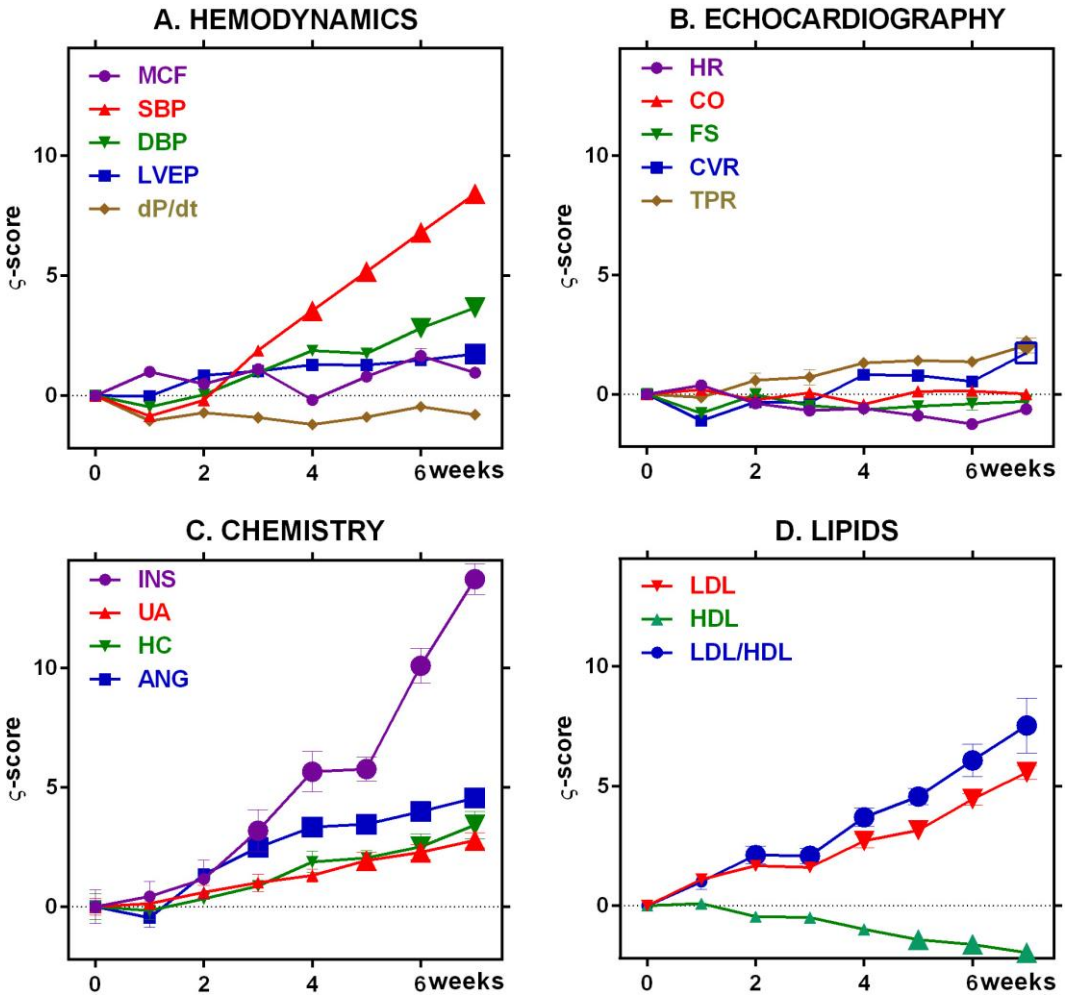

Fig. 3. Evolution of hemodynamics, echocardiographic characteristics and levels of hormones and lipids during the 7 weeks high fructose feeding of 6 adult male dogs. Numbers after feature acronyms are the average ± sd of the absolute control values (i.e. before starting the fructose diet). Data were normalized and transformed to numbers. Larger symbols indicate ($p < 0.05$) significant regulation with respect to control. Data were plotted on the same scale to compare the alterations of various features.

From the ζ-score perspective, increase of INS (ζ = 13.71), SBP (8.42) and LDL/HDL increase (7.53) had the highest impact on the dog health. However, none of these reported altered features exhibited any saturation and more alteration is expected if the fructose-feeding continued beyond the 7 weeks.

We found that more features became altered when the duration of fructose feeding increases. Insulin (**INS**) had the largest alteration (ζ = 13.71) after 7 weeks fructose and **MCF**, **dP/dt**, **CO** and **HR** were not significantly altered at any time during this period. The difference between the levels of low (LDL) and high density (HDL) lipids was also plotted owing to its own clinical significance beyond the levels of the two components.

3.3. Correlation of pathophysiological features

No significant correlation was found between variations of MCF, SBP, DBP, LVEP, dP/dt, HR, CO, FS, CVR, TPR, INS, UA, HC, ANG, LDL and HDL in any condition. Therefore, all of these variables were considered as independent and the pre-Hilbert space of states was constructed with them. However, SBP, DBP, INS, UA, HC and LDL/HDL exhibited correlated increase in their absolute values during fructose-feeding (Fig. 4).

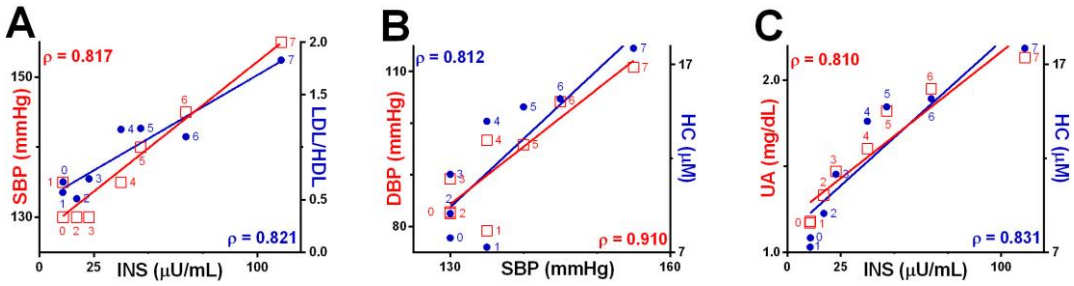

Fig.4. Correlated increase of hemodynamics, chemistry and low-to-high lipid density ratio during fructose feeding. ρ = pair-wise Pearson correlation coefficient between the average (for the six dogs) increase of the feature represented on x-axis and those of the features represented on the left and right axes. 0, 1, 2 , … close to symbols indicate the number of weeks of fructose feeding. Note the significant correlated increase of these features.

3.4. The pre-Hilbert space of pathological states

Figure 5A presents a 3D section (systolic blood pressure, difference between the plasma levels low and high density lipids and insulin level) from the space of states. Figure 5B illustrates the 7-week dynamics of the patholog and Figure 5C presents the 7-week dynamics of the standard patholog.

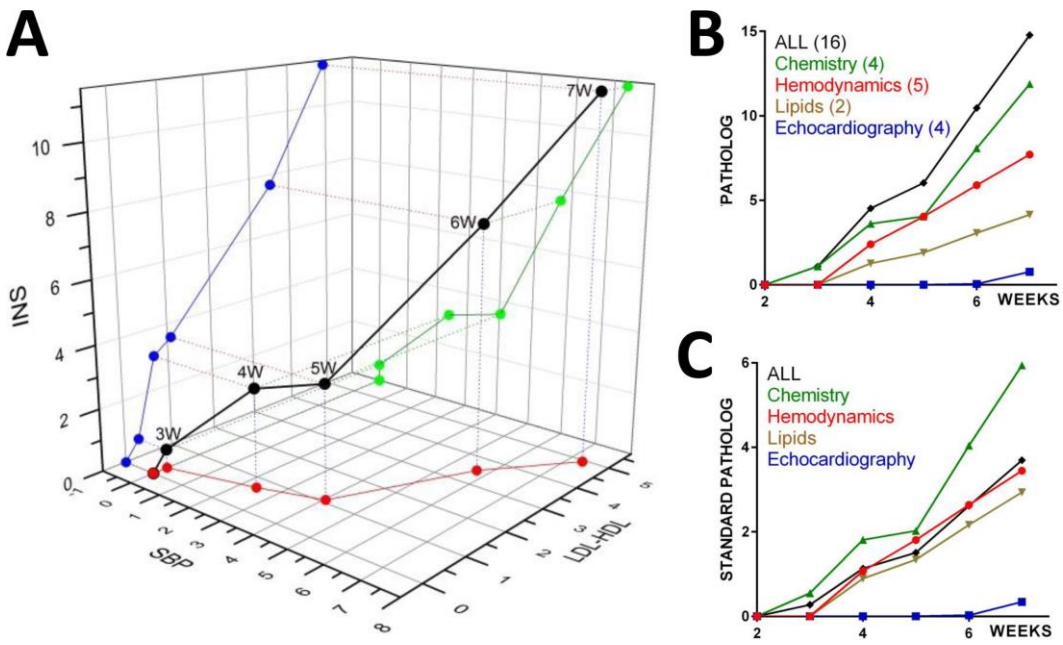

Fig. 5. A. 3D section through the pre-Hilbert of states of a group of 6 adult male dogs subjected for 0, 1, …, 7 weeks to 60% isocaloric fructose diet (note the projections in the 2D planes)**.** Patholog for each time point with respect to these variables is the distance from the origin. **B. Evolution of the patholog of all and subsets of features.** Numbers indicate how many independent features were considered in each set. The plot started after the second week of fructose feeding since no pathologic alteration was recorded for one week. Note that although the MetS was installed after 4 weeks fructose feeding, the patholog more than doubled after other 3 weeks fructose, without any indication of saturation. **C. Evolution of the standard patholog for all and subset of features.** Note that the largest alteration is associated with changes in hormones' levels.

Conclusions

The **dog** was the first and it is still the most used large animal model for the human cardiovascular diseases (>54,000 published studies on canine models). However, dog's heart is highly aerobic and very exercise tolerant, and metabolism evolution has favored protein diet as opposed to the humans which are omnivores. Although the Ossabaw pig model may be a better representation of genetically disposed human MetS [35-37], we have preferred the dog because it can be trained, allowing studies on previously instrumented, conscious animals with no anesthetic effects on the cardiovascular physiology [24-29].

We have observed that decrease of the insulin level is associated with increase of the half-life of the administrated glucose in the glucose tolerance test (Fig. 1). This expected observation led to a very simple and intuitive measure for the **insulin resistance** by linking the blood level of insulin to the decay of glucose level in the glucose tolerance test. Possible (not mutually exclusive) causes of the much faster increase of *IR* than of

[INS] include: i) saturation of insulin receptors, ii) reduction of insulin receptors or iii) alteration of insulin signaling pathway. An RNA-sequencing experiment is underway to check the last two potential causes at the transcriptomic level of the left ventricle. However, [INS] was not measured during the 75-min glucose tolerance test. Therefore, experimental data cannot be used in mechanistic models of insulin sensitivity in dogs subjected to intravenous glucose tolerance tests [38] or other "minimal models" [39] seeking fitting of experimental curves.

Our **mathematical approach** with the "patholog" as a global quantifier offers the simplest, yet the most intuitive way to quantify and compare the effects of altering individual and combined features of wide diversity. Thus, if a feature is of higher importance, then the homeostatic mechanisms will keep its value (expression level for genes) within a narrow interval. Therefore, the ς-transformation made *comparable the effects of altered characteristics* regardless of their different nature and measuring scale. For instance, 131.5 mmHg for SBP (i.e. an increase with 7% from the control 123 ± 4 mmHg in Fig. 2) has the same $\varsigma = 2$ score as 29.0 μU/mL for INS (+141%), 195.9 mg/dL for HDL (+44%) or 2.0 mg/dL for UA (+70%). Moreover, the score ς is independent on the scale used for the absolute values: e.g. $\varsigma = 2$ for both 37.8°C (an increase with 2.2% from the normal 37.0 ± 0.4°C) and 100.0°F (+ 1.0% from the normal or 98.6 ± 0.7°F) in the case of orally taken body temperature.

With the "patholog" values determined before and after a treatment (Θ) one can compute the **efficacy** *E* **of that treatment** as the percent reduction of the "patholog":

$$E(\Theta) = \left(1 - \frac{\Psi_{after\,\Theta}}{\Psi_{before\,\Theta}}\right) \times 100\% \tag{8}$$

Such definition offers an objective score of the global amelioration of the disease-induced changes of physiological features. From this perspective, the possible outcomes are:

1) $E = 100\% \leftarrow \Psi_{after} = 0$ (cured)
2) $0 < E < 100\% \leftarrow 0 < \Psi_{after} < \Psi_{before}$ (ameliorated)
3) $E = 0 \leftarrow \Psi_{after} = \Psi_{before}$ (null)
4) $E < 0 \leftarrow \Psi_{after} > \Psi_{before}$ (negative)

Outcome (2) does not mean necessarily that the "after" state is identical to the "before" one. Instead, it means that the representative points are on the same 0-centered hypersphere (hence equal distance to the center, i.e. physiological state).

In summary, our approach is the simplest (yet strong enough) one can imagine to globally quantify the evolution of a disease and result of a treatment.

Notations
CVR = coronary vascular resistance
dp/dt = rate of LV pressure rise
FS = fractional shortening

HDL = high density lipids ("good" cholesterol)
HFD = high fructose diet
IR = insulin resistance
LAD = left anterior descending
LDL = low density lipids ("bad" cholesterol)
LV = left ventricle
LVDD = left ventricle diameter in diastole
LVDS = left ventricle diameter in systole
MAP = mean arterial pressure
MCF = mean coronary flow
MetS = Metabolic syndrome
RCA = right coronary artery

R E F E R E N C E S

[1]. Johnson RK, Appel LJ, Brands M, Howard BV, Lefevre M, Lustig RH, et al. American Heart Association Nutrition Committee of the Council on Nutrition, Physical Activity, and Metabolism and the Council on Epidemiology and Prevention. Dietary sugars intake and cardiovascular health: a scientific statement from the American Heart Association. *Circulation* 2009; **120**(11):1011-1020.
[2]. Kelishadi R, Mansourian M, Heidari-Beni M. Association of fructose consumption and components of metabolic syndrome in human studies: a systematic review and meta-analysis. *Nutrition*. 2014 **30**(5):503-10. Review.
[3]. Sloboda DM, Li M, Patel R, Clayton ZE, Yap C, Vickers MH. Early life exposure to fructose and offspring phenotype: implications for long term metabolic homeostasis. *J Obes*. 2014;2014:203474. Review.
[4]. Yracheta JM, Alfonso J, Lanaspa MA, Roncal-Jimenez C, Johnson SB, Sánchez-Lozada LG, et al. Hispanic Americans living in the United States and their risk for obesity, diabetes and kidney disease: Genetic and environmental considerations. *Postgrad Med.* 2015;**127**(5):503-10.
[5]. Lakka HM, Laaksonen DE, Lakka TA, Niskanen LK, Kumpusalo E, Tuomilehto J, et al. The metabolic syndrome and total and cardiovascular disease mortality in middle-aged men. *JAMA*. 2002; 288(21):2709-2716.
[6]. Alberti KG, Zimmet P, Shaw J. IDF Epidemiology Task Force Consensus Group. The metabolic syndrome--a new worldwide definition. *Lancet*. 2005; 366(9491):1059-1062.
[7]. Ferder L, Ferder MD, Inserra F. The role of high fructose corn syrup in metabolic syndrome and hypertension. *Current Hypertension Research* 2010; 12:105-112.
[8]. Seneff S, Wainwright G, Mascitelli L. (2011). Is the metabolic syndrome caused by a high fructose, and relatively low fat, low cholesterol diet? *Arch Med Sci*. 7(1):8-20.
[9]. Ha V, Jayalath VH, Cozma AI, Mirrahimi A, de Souza RJ, Sievenpiper JL. Fructose-containing sugars, blood pressure, and cardiometabolic risk: a critical review. *Curr Hypertens Rep*. 2013; 15(4):281-97.
[10]. Ford ES. Prevalence of the metabolic syndrome defined by the International Diabetes Federation among adults in the U.S. *Diabetes Care* 2005; 28(11):2745-2749.
[11]. Dai S, McNeill JH. Fructose-induced hypertension in rats is concentration- and duration-d9pendent. *J Pharmacol Toxicol Methods* 1995; 33(2):101-107.
[12]. Suzuki M, Yamamoto D, Suzuki T, Fujii M, Suzuki N, Fujishiro M, Sakurai T, Yamada K. High fat and high fructose diet induced intracranial atherosclerosis and enhanced vasoconstrictor responses in non-human primate. *Life Sci* 2006; 80(3):200-204.

[13]. Stirpe F, Della Corte E, Bonetti E, Abbondanza A, Abbati A, De Stefano F. Fructose-induced hyperuricaemia. *Lancet*. 1970; 2(7686):1310-1311.
[14]. Tappy L, Le KA. Metabolic effects of fructose and the world wide increase in obesity. *Physiol Rev* 2010; 90(1):23-46.
[15]. Stanhope KL, Havel PJ. Fructose consumption: potential mechanisms for its effects to increase visceral adiposity and induce dyslipidemia and insulin resistance. *Curr Opin Lipidol*. 2008; 19(1):16-24.
[16]. Lê KA, Ith M, Kreis R, Faeh D, Bortolotti M, Tran C, Boesch C, Tappy L. Fructose overconsumption causes dyslipidemia and ectopic lipid deposition in healthy subjects with and without a family history of type 2 diabetes. *Am J Clin Nutr*. 2009; 89(6):1760-1765.
[17]. Vos MB, Kimmons JE, Gillespie C, Welsh J, Blanck HM. Dietary Fructose Consumption Among US Children and Adults: The Third National Health and Nutrition Examination Survey. *Medscape J Med*. 2008; 10(7):160.
[18]. Hwang IS, Ho H, Hoffman BB, Reaven GM. Fructose-induced insulin resistance and hypertension in rats. *Hypertension*. 1987; 10(5):512-516.
[19]. Martinez FJ, Rizza RA, Romero JC. High-fructose feeding elicits insulin resistance, hyperinsulinism, and hypertension in normal mongrel dogs. *Hypertension*. 1994; 23(4):456-63.
[20]. Elliott SS, Keim NL, Stern JS, Teff K, Havel PJ. Fructose, weight gain, and the insulin resistance syndrome. *Am J Clin Nutr*. 2002; 76(5):911-922.
[21]. Teff KL, Elliott SS, Tschop M, Kieffer TJ, Rader D, Heiman M, Townsend RR, Keim NL, D'Alessio D, Havel PJ. Dietary fructose reduces circulating insulin and leptin, attenuates postprandial suppression of ghrelin, and increases triglycerides in women. *J Clin Endocrinol Metab*. 2004; 89(6):2963-2972.
[22]. Shapiro A, Mu W, Roncal C, Cheng KY, Johnson RJ, Scarpace PJ. Fructose-induced leptin resistance exacerbates weight gain in response to subsequent high-fat feeding. *Am J Physiol Regul Integr Comp Physiol* 2008; 295(5):R1370-5.
[23]. Shapiro A, Tümer N, Gao Y, Cheng KY, Scarpace PJ. Prevention and reversal of diet-induced leptin resistance with a sugar-free diet despite high fat content. *Br J Nutr*. 2011; 106(3):390-7.
[24]. Wang J, Wolin MS, Hintze TH. Chronic exercise enhances endothelium-mediated dilation of epicardial coronary artery in conscious dogs. *Circ Res* 1993; 73:829-838.
[25]. Bernstein RD, Ochoa FY, Xu X, Forfia P, Shen W, Thompson CI, Hintze TH. Function and production of nitric oxide in the coronary circulation of the conscious dog during exercise. *Circ Res*. 1996; 79(4):840-8. Erratum in: *Circ Res* 199; 79(6):1218.
[26]. Zhao G, Zhang X, Smith CJ, Xu X, Ochoa M, Greenhouse D, Vogel T, Curran C, Hintze TH. Reduced coronary NO production in conscious dogs after the development of alloxan-induced diabetes. Am J Physiol. 1999; 277: H268–H278.
[27]. Vimercati C, Qanud K, Mitacchione G, Sosnowska D, Ungvari Z, Sarnari R, Mania D, Patel N, Hintze TH, Gupte SA, Stanley WC, Recchia FA. Beneficial effects of acute inhibition of the oxidative pentose phosphate pathway in the failing heart. Am J Physiol Heart Circ Physiol. 2014, 306(5):H709-17.
[28]. Nganele DM, Hintze TH. Cardiac chemical reflex control of preload in conscious dogs. *Am J Physiol.* 1990; 258(4 Pt 2):H1055-63.
[29]. Becker JS, Adler A, Schneeberger A, Huang H, Wang Z, Walsh E, Koller A, Hintze TH. Hyperhomocysteinemia, a cardiac metabolic disease: role of nitric oxide and the p22phox subunit of NADPH oxidase. Circulation 111: 2112-2118, 2005.
[30]. Johnson, Norman L.; Kotz, Samuel; Balakrishnan, N. (1994), "14: Lognormal Distributions", Continuous univariate distributions. Vol. 1, Wiley Series in Probability and Mathematical Statistics: Applied Probability and Statistics (2nd ed.), New York: John Wiley & Sons
[31]. Iacobas DA. *Medical Biostatistics* 3rd edition (Bucura Mond, Bucharest, 1997)

[32]. Iacobas DA, Iacobas S, Lee PR, Cohen JE, Fields RD. Coordinated Activity of Transcriptional Networks Responding to the Pattern of Action Potential Firing in Neurons. *Genes* **10**(10), 754 (2019). https://doi.org/10.3390/genes10100754.
[33]. Iacobas S, Iacobas DA. A mathematical transcription of a current problem in physiology. *Physiologie* **24**(4):263-5 (1987).
[34]. Iacobas DA. Ideas and Methods in the Physics of the Living, 4th English edition. (Constanta: Tilia Press Intl. Ltd. (2000)
[35]. Spurlock ME, Gabler NK. The development of porcine models of obesity and the metabolic syndrome. *J Nutr*. 2008; 138(2):397-402.
[36]. Litten-Brown JC, Corson AM, Clarke L. Porcine models for the metabolic syndrome, digestive and bone disorders: a general overview. *Animal*. 2010; **4**(6):899-920.
[37]. Li ZL, Woollard JR, Ebrahimi B, Crane JA, Jordan KL, Lerman A, Wang SM, Lerman LO. Transition from obesity to metabolic syndrome is associated with altered myocardial autophagy and apoptosis. *Arterioscler Thromb Vasc Biol.* 2012; 32(5):1132-41.
[38]. Bergman RN, Ider YZ, Bowden CR, Cobelli C. Quantitative estimation of insulin sensitivity. *Am J Physiol.* 1979; 236(6):E667-77.
[39]. Caumo A, Bergman RN, Cobelli C. Insulin sensitivity from meal tolerance tests in normal subjects: a minimal model index. *J Clin Endocrinol Metab.* 2000; **85**(11):4396-402.